JOURNAL OF MATERIALS SCIENCE 31 (1996) 2603–2607

Chemical processing and characterization of spinel-type thermistor powder in the Mn–Ni–Fe oxide system

Y. TORII, A. TSUZUKI, K. KATO, Y. UWAMINO
National Industrial Research Institute of Nagoya, Hirate-cho, Kita-ku, Nagoya 462, Japan
B. H. CHOI, M. J. LEE
Institute of Ceramic Technology, 233-5, Gasan-Dong, Gyumcheon-ku, Seoul, Korea

The coprecipitated Mn–Ni–Fe oxalate was prepared from the mixed sulfate solution by optimum pH control. The chemical composition agreed well with that of the starting solution, and the thermal decomposition of the Mn–Ni–Fe oxalate in air below 600 °C led to the direct formation of cubic spinel phase with fine particle size. The sinterability of the calcined powder, the stability of cubic spinel phase and the influence of annealing temperature on electrical properties of the sintered bodies, were investigated.

1. Introduction

Thermistors with a negative temperature coefficient (NTC) are widely used for electronic applications. Such semiconducting ceramics are most often constituted of spinel phases mainly in the Mn–Ni oxide system. The electrical properties, for example, resistivity and stability, depend on several parameters such as the composition, purity, cation distribution and microstructural development, etc. [1]. In the fabrication of NTC thermistors, it is especially important to reproduce reliable electrical characteristics, e.g. resistivity at room temperature and thermistor B constant. The first step to solve this problem is to prepare chemically homogeneous powders of monophase spinel.

Coprecipitation is an attractive method for producing fine powders because of increased homogeneity, purity, and reactivity over standard ceramic processing. The chemical species most frequently used are the hydroxides [2, 3], oxalates [4, 5], and carbonates [6]. However, the hydroxides are gelatinous, leading to difficulty with filteration. In addition, loss of some ions by complexing occurs, when ammonia is the precipitant. The carbonates give poor sinterability after decomposition. In this respect, the powders obtained from oxalates have the advantage that they can be more readily handled and require far less washing than the coprecipitated hydroxides. In the case of soft ferrites, the Ni–Fe oxalates have been reported to be coprecipitated on admixing ammonium oxalate in the aqueous sulfate solution. However, the precipitation of transition metal ions is known to be incomplete on complexing with free NH_4^- ion when the pH is high. No detailed report has been published on the oxalate coprecipitation for manganite-based spinel thermistors. One means of preventing the complexing is considered to be the formation of the coprecipitated oxalate at low pH.

In the present work, a sample composition with a Mn/Ni/Fe ratio of 2.1/0.6/0.3 was selected, which is close to that of a thermistor currently on the market. The coprecipitated oxalate was prepared by slowly adding ammonia water into the slurry solution of the oxalate coprecipitated only with oxalic acid, and the relation between pH and the chemical composition of the final coprecipitates was examined. In addition, the thermal decomposition of the coprecipitated oxalate, the sintering behaviour of calcined powder, the high-temperature stability of cubic spinel phase, and the influence of annealing temperature on thermistor characteristics of the sintered bodies were investigated.

2. Experimental procedure

An aqueous sulfate solution of manganese, nickel and iron was mixed to give the desired molar ratio, and a 1.80 M master solution of combined divalent metal sulfates was then prepared with distilled water. Firstly, a 70 ml solution of mixed divalent sulfates was added to 100 ml of vigorously stirred solution of 1.51 M oxalic acid at room temperature, and the resulting slurry was stirred for 1 h and then left overnight. Then the pH of the slurry solution was about 0.5. After stirring again for 1 h, triply diluted ammonia water was slowly added to the stirred slurry solution of coprecipitated oxalate at the pH range of 0.9–3.3. The yellow–green crystalline precipitates were filtered, washed with chilled water and dried at 80 °C in air.

The X-ray diffraction method was used to follow the conversion of the oxalate to the desired spinel phase. Differential thermal analysis (DTA) and thermogravimetry (TG) curves were measured in air at a heating rate of 10 °C min^{-1} in order to investigate the thermal decomposition behaviour of the coprecipitated oxalate.

0022–2461 © *1996 Chapman & Hall*

Electrical resistivity of the sintered bodies was measured in air between room temperature and 400 °C using silver paste as electrodes, which is fired at 820 °C to make good ohmic contacts to the sintered bodies.

3. Results and discussion

The individual dissolved metals lost in the filtrate were quantitatively determined by ICP analysis. Fig. 1 shows the variation of the percentage of each metal precipitated from the mixed sulfate solution as a function of the final pH. The nickel ion was almost perfectly precipitated in this pH range. About 98% iron ions were precipitated at pH = 1.5–2.0, and the amount of precipitated iron decreased at pH > 2.1. On the other hand, only 74% manganese ions were precipitated at pH = 0.54. The precipitated manganese yield was remarkably improved by adding ammonia water into the slurry solution, and the amount reached 98% at pH = 2.5. Consequently, the optimum condition for the coprecipitation was concluded to be about pH = 2.5. The ICP analysis of the dried coprecipitate, which was prepared at pH = 2.5, showed the chemical composition with a molar ratio of Mn/Ni/Fe = 69.3/20.5/10.1 and agreed well with that (70.6/19.6/9.8) of the starting solution. Fig. 2 shows a scanning electron micrograph of the oxalate powder. The aggregated powder consisted of platelet particles.

Fig. 3 shows the TG–DTA curve for the coprecipitated Mn–Ni–Fe oxalate (pH = 2.5) dried at 80 °C. Two steps of weight loss were observed at 140–235 °C and 265–305 °C. They correspond to the dehydration of oxalate and the decomposition of anhydrous oxalate, respectively. On the other hand, a sharp exothermic peak appeared around 297 °C, followed by an endothermic peak around 235 °C. The TG–DTA curve for the mechanical mixture of individual metal oxalates with the same composition as the Mn–Ni–Fe coprecipitate is given in Fig. 4 for comparison. The exothermic peaks were separately observed around 246, 291 and 362 °C, which correspond to the decomposition of iron, manganese and nickel anhydrous oxalates, respectively. Thus there are obvious differences in the coprecipitated oxalate and the mechanical mixture with the same composition. The fact that the coprecipitated oxalate seems to behave as a single entity is proof that the nickel and iron ions coprecipitate in the solid solution form of (NiFeMn)$(C_2O_4)_2 \cdot 2H_2O$, although a small amount of manganese oxalate may be dispersed in the dried oxalate coprecipitate.

Fig. 5 shows the XRD patterns of samples decomposed at 400–1000 °C for 3 h in air. The XRD pattern characteristic of spinel structure was observed when fired even at 400 °C. The reflections became strong and sharp when fired at 600 and 800 °C, and was clearly indexed as a cubic spinel monophase. Fig. 6 shows a scanning electron micrograph of cubic spinel powder calcined at 900 °C for 3 h in air. The calcined powder is aggregated with the individual particles of about 3 μm in size. In the usual mixed-oxide process, the reaction of NiO with Mn_2O_3 was scarcely observed in firing at 800 °C for 3 h, and it needs heat treatment at 1000–1200 °C to obtain the monophase spinel, as shown in Fig. 7. Thus the oxalate coprecipitation method based on pH control is effective for

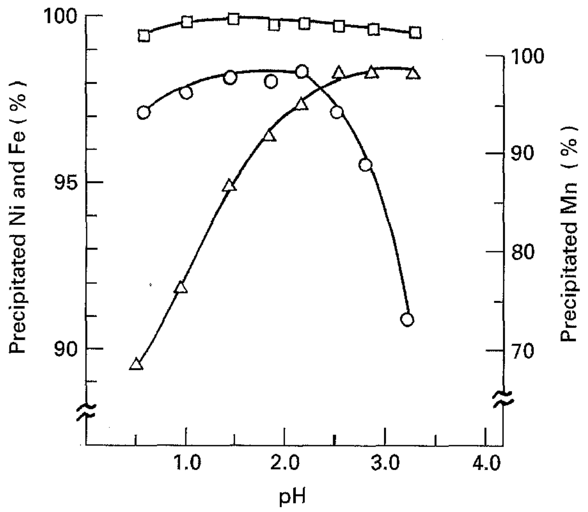

Figure 1 Influence of pH for the oxalate coprecipitation of each cation. (□) Ni, (○) Fe, (△) Mn.

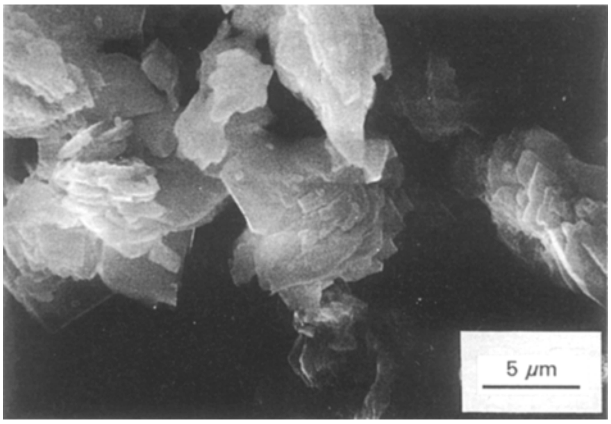

Figure 2 Scanning electron micrograph of coprecipitated oxalate powder.

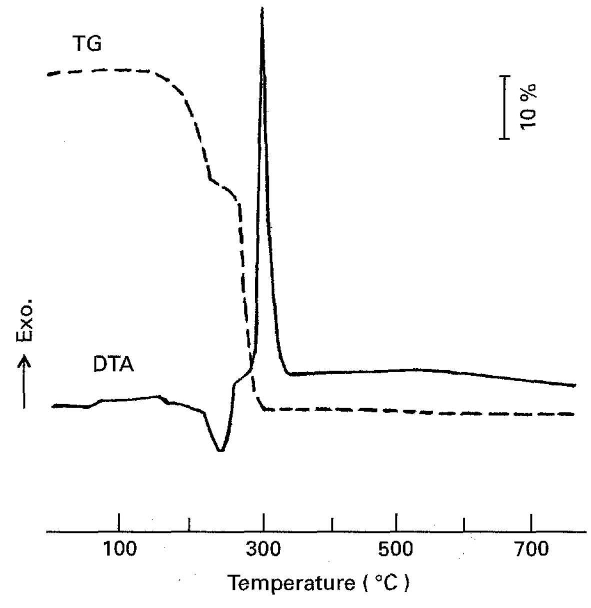

Figure 3 TG–DTA curve for coprecipitated Mn–Ni–Fe oxalate.

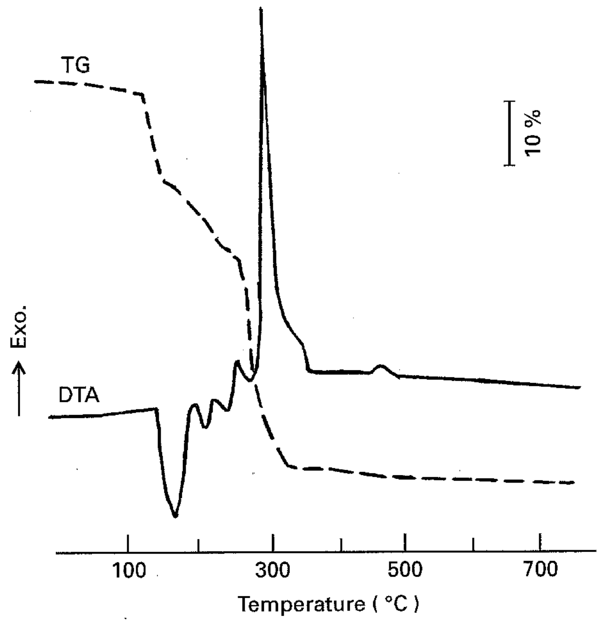

Figure 4 TG–DTA curve for the mixture of individual oxalates.

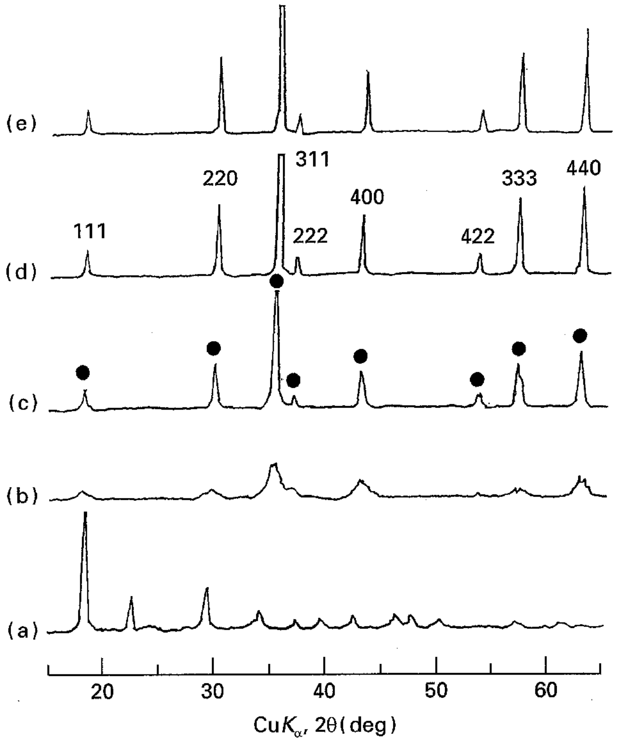

Figure 5 XRD patterns for samples prepared from coprecipitated oxalate at various temperatures for 3 h: (a) original, (b) 400 °C, (c) 600 °C, (d) 800 °C, and (e) 1000 °C. (●) Spinel.

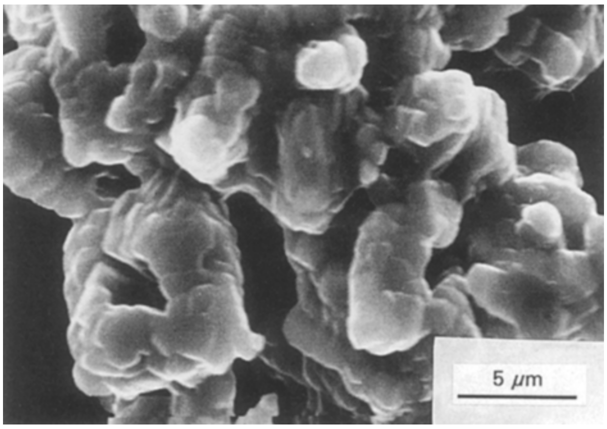

Figure 6 Scanning electron micrograph of cubic spinel powder calcined at 900 °C for 3 h.

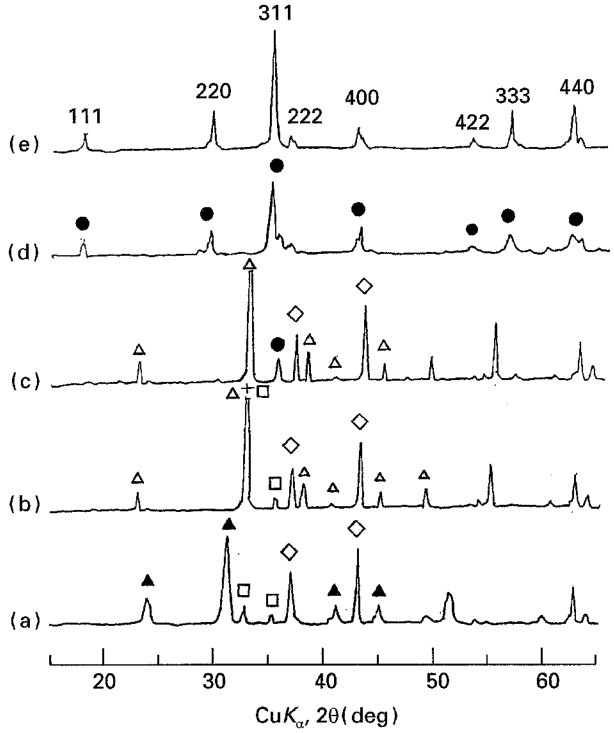

Figure 7 XRD patterns for samples prepared from oxides and carbonate at various temperatures for 3 h: (a) original, (b) 600 °C, (c) 800 °C, (d) 1000 °C, and (e) 1200 °C. (●) Spinel, (△) Mn_2O_3, (◇) NiO, (▲) $MnCO_3$, (□) Fe_2O_3.

producing fine powders for spinel thermistors at relatively low temperature. The powder calcined at 900 °C for 3 h was used for the measurement of relative density and electrical properties of the sintered bodies.

Fig. 8 shows the change in relative density of the sintered bodies with firing temperature. The green compacts were well densified when fired at 1300–1400 °C, and the relative density reached about 95% maximum. The body sintered at 1400 °C for 5 h, however, showed the significant decrease of relative density. This suggests that phase change occurs during the sintering. In fact, a slight amount of rock salt-type NiO phase was observed in the XRD pattern. When quenched after firing at 1350 or 1400 °C for 24 h, tetragonal spinel and NiO coexisted together with the cubic spinel, as expected from partial phase diagram for the $Ni_{1-x}Mn_{2+x}O_4$ system [7]. This tetragonal spinel is manganese-rich as compared with the initial cubic spinel. Remarkably, the tetragonal phase formed when quenched at 1400 °C and had a large crystal distortion ($c/a = 1.06$) based on the Jahn–Teller effect of Mn^{3+} ions in the octahedral site. When quenched at 1300 and 1325 °C, however, only the cubic spinel was observed in the XRD patterns. The temperature at which phase separation occurs depends on the spinel composition, and the green body must be sintered below 1325 °C in order to obtain the monophase

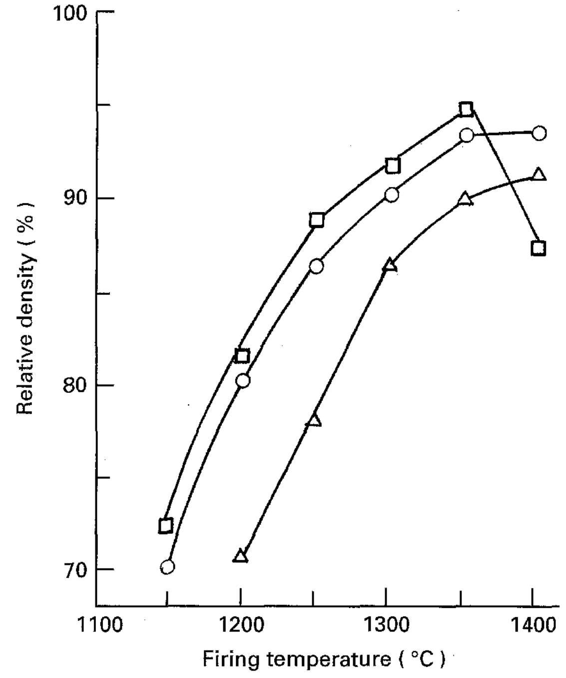

Figure 8 Change in relative density of sintered bodies with firing temperature. (□) 5 h, (○) 3 h, (△) 1 h.

of cubic spinel at this composition. The phase-separation temperature is about 100 °C higher compared with that (≃1230 °C) in the cubic spinel of $Ni_{0.6}Mn_{2.4}O_4$. Therefore, the iron ions in $Ni_{0.6}Fe_{0.3}Mn_{2.1}O_4$ are considered to make a significant contribution to the stabilization of cubic spinel structure. Fig. 9 shows the microstructure of the sample fired at 1300 °C for 5 h. The relative density is 92%, and the grains are about 10–30 μm in size. Small pores are often observed only at triple grain junctions.

The stability of the cubic spinel phase at 400–1000 °C in air was also examined, because Mn_3O_4 is well known to be in equilibrium with Mn_2O_3 at 885 °C in air. As a result, a certain amount of Mn_2O_3 phase was observed in the XRD patterns only when annealed at 500–700 °C for 24 h. This indicates that the manganite-based cubic spinel is locally oxidized to form Mn_2O_3 phase. To reproduce reliable NTC characteristics, much attention should be given to process control in the moderate temperature region during cooling after sintering and electroding.

Fig. 10 shows the temperature dependence of resistivity for the sample sintered at 1325 °C for 5 h. The data points lie perfectly on a straight line determined by the least square method. The thermistor constants were determined to be $\rho_{25} = 6278$ Ωcm and $B = 4126$ K, respectively. The electrical data for the sample annealed at 1100 °C for 5 h are also given for comparison.

Fig. 11 shows the changes in resistivity at room temperature and the B constant when sintered at 1325 °C for 5 h and then annealed at varied temperatures for 7 h. The ρ_{25} remains unchanged for annealing below 500 °C, increased when annealed at 600 and 700 °C, and decreased rapidly on annealing above 800 °C. The ρ_{25} of the sample annealed at 1100 °C was lower, by 32%, than that of the as-fired sample. On the other hand, B increased when annealed at 500–700 °C and then decreased when annealed above 800 °C. For the sample annealed at 1100 °C, B was 2.3% lower than that of the as-fired sample. In conclusion, the change in B is very much smaller than that in the value

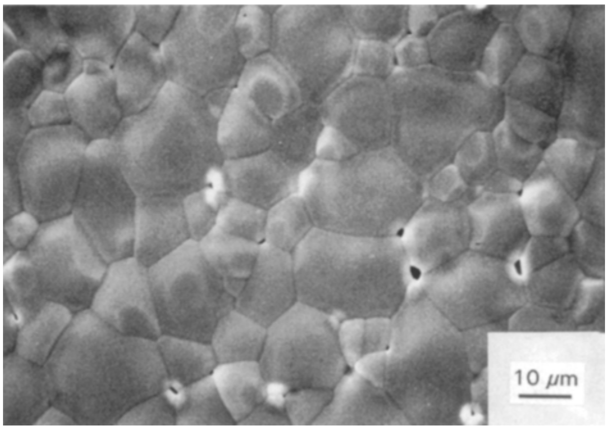

Figure 9 Microstructure of the cubic spinel body fired at 1300 °C for 5 h.

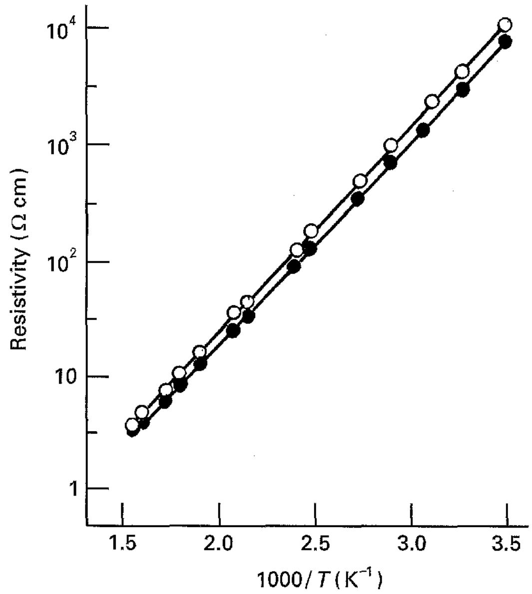

Figure 10 Temperature dependence of resistivity for thermistor bodies sintered at 1325 °C for 5 h (○) and then annealed at 1100 °C for 7 h (●).

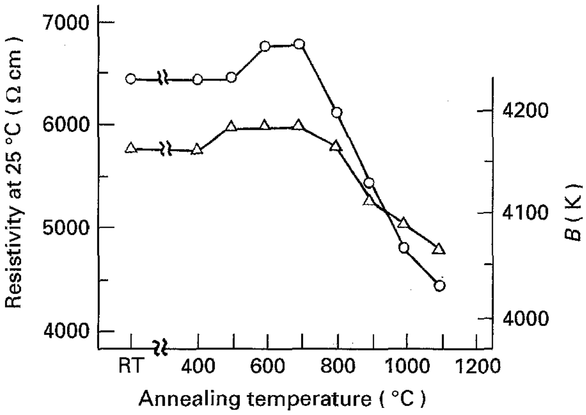

Figure 11 Influence of annealing temperature on (○) ρ_{25} and (△) B constant for the bodies fired at 1325 °C for 5 h.

of ρ_{25}, and annealing should be avoided in the temperature region of 500–800 °C.

4. Conclusion

The coprecipitated Mn–Ni–Fe oxalates were prepared from mixed sulfate solution. The chemical composition of the coprecipitated oxalate was found to agree well with that of the starting solution by optimum pH control. The atomic-scale mixing in the salt crystal enabled the direct formation of spinel of fine particle size. The sample fired at 1350 °C for 5 h had a relative density of about 95%.

The manganite-based cubic spinel was not stable at high temperatures and, when fired above 1350 °C and then quenched in air, was reduced to form manganese-rich tetragonal spinel and rock salt-type NiO phase. However, the iron ions in $Ni_{0.6}Fe_{0.3}Mn_{2.1}O_4$ were found to make a significant contribution to the stabilization of cubic spinel structure.

On annealing at 500–700 °C for 24 h, on the other hand, the manganite-based cubic spinel was locally oxidized to form Mn_2O_3 phase. This seems to be reflected in the changes in ρ_{25} and B constant with annealing temperature. On the whole, the influence of annealing temperature on thermistor characteristics was large in the ρ_{25} value.

References

1. J. K. FAGAN and V. R. W. AMARAKOON, *Am. Ceram. Soc. Bull.* **72** (1993) 70.
2. D. W. JOHNSON, *ibid.* **60** (1981) 221.
3. P. K. GALLAGHER and F. SCHREY, *J. Am. Ceram. Soc.* **47** (1964) 434.
4. P. K. GALLAGHER, H. M. O'BRYAN, F. SCHREY and F. R. MONFORTE, *Am. Ceram. Soc. Bull.* **48** (1969) 1053.
5. R. LEGROS, R. METZ, J. P. CAFFIN, A. LAGRANGE and A. ROUSSET, *Mater. Res. Symp. Proc.* **121** (1988) 251.
6. A. GOLDMAN and A. M. LAING, *J. de Phys.* **38** (1977) 297.
7. E. G. LASON, R. J. ARNOTT and D. G. WICKHAM, *J. Phys. Chem. Soc.* **23** (1962) 1771.

Received 25 April 1995
and accepted 3 November 1995